Materials Science-Poland, *Vol. 27*, *No. 3*, *2009*

Optical study of β″-(bis(ethylenedithio)tetrathiafulvalene)$_2SF_5CH_2SO_3$ Activation of intramolecular modes*

I. OLEJNICZAK[1**], B. BARSZCZ[1], A. GRAJA[1], J.A. SCHLUETER[2]

[1]Institute of Molecular Physics, Polish Academy of Sciences,
Smoluchowskiego 17, 60-179 Poznań, Poland

[2]Materials Science Divisions, Argonne National Laboratory, Argonne, Illinois 60439-4831, USA

We report on the temperature dependences of polarized reflectance spectra of β″-(bis(ethylenedithio)tetrathiafulvalene)$_2SF_5CH_2SO_3$. The material remains in the charge-ordered state over the whole temperature range. Room temperature infrared spectra display the response characteristic of a quasi-two-dimensional organic conductor, with a broad mid-infrared electronic excitation and a number of vibrational features related to intramolecular modes of both the bis(ethylenedithio)tetrathiafulvalene (ET) donor molecule and the $SF_5CH_2SO_3$ anion. Upon lowering the temperature, unusual activation of intramolecular modes of ET is observed. We suggest that this effect is connected with electron-molecular vibration coupling within a dimerized lattice.

Key words: *BEDT-TTF; oganic conductor; reflectance spectra; electron–phonon interactions; charge ordering*

1. Introduction

Quasi-two-dimensional organic conductors based on the organic donor molecule of bis(ethylenedithio)tetrathiafulvalene (ET) are widely regarded as good model compounds to study broken symmetry ground states [1]. Extensive experimental studies of these materials have been stimulated by the discovery of superconductivity and other competing ground states that are related to a complex interplay of charge, spin and vibrational degrees of freedom. In particular, the procedure of incorporating large, discrete, chemically tunable anions within an ET framework resulted in the family

---

*The paper presented at the 11th International Conference on Electrical and Related Properties of Organic Solids (ERPOS-11), July 13–17, 2008, Piechowice, Poland.

**Corresponding author, e-mail: ywy@ifmpan.poznan.pl

β″-$(ET)_2SF_5RSO_3$ (R = CH_2CF_2, $CHFCF_2$, or CHF), where superconducting, semiconducting, or metallic ground states have been realized depending on R [2, 3]. β″-$(ET)_2SF_5CH_2SO_3$ is another example of a salt synthesized based on ET and pentafluorothiomethylsulfonate anions being of interest here.

The crystal structure of β″-$(ET)_2SF_5CH_2SO_3$ consists of alternating layers of ET cations and $SF_5CH_2SO_3^-$ anions [4]. ET molecules in the donor layer form stacks along the *a* direction. Short intermolecular S···S contacts* are found between adjacent donor stacks but not within stacks. F and O atoms of the anion make numerous contacts with ethylene hydrogen atoms of donor molecules. Also, C–H···O hydrogen bond interactions occur between anions. The unit cell is composed of four ETs, forming one conducting plane, and has an inversion centre, therefore there are two pairs of equivalent ETs. Non-equivalent ET molecules are characterized by different patterns of short contacts with the anion layer, and also different charge, which was estimated 0.6 and 0.4, based on the structure [4]. Such a charge localization results in semiconducting properties, although typical β″-type quarter-filled systems are usually two-dimensional metals.

In this paper, we present polarized reflectance spectra of β″-$(ET)_2SF_5CH_2SO_3$, measured as a function of temperature in order to gain further information on the nature of electronic processes in the β″-phase materials with highly tunable organic anions. In our experiment, we concentrate on intramolecular vibrational modes of the ET molecule, which strongly appear in the spectra upon lowering the temperature.

2. Experimental

High-quality single crystals of β″-$(ET)_2SF_5CH_2SO_3$ were grown using electrochemical techniques in an H-cell [4]. For infrared measurements we used a 3.5×2×0.4 mm^3 plate sample. Optical axes were defined as those displaying the largest anisotropy at 300 K. Two directions within the conducting plane were probed; the ∥*b* direction of maximum reflectance, and the ⊥*b* direction, which is close to the ET stack of the *a* direction. Polarized infrared reflectance measurements (600–7000 cm^{-1}) were performed using a Perkin Elmer 1725 X Fourier-transform infrared spectrometer, equipped with an Olympus infrared microscope and a polarized gold grid. The sample was cooled from room temperature down to 10 K using an Oxford Instruments continuous-flow cryostat. Additionally, the 300 K polarized reflectance spectra were recorded using a Bruker Equinox 55 FT-IR spectrometer equipped with a Bruker IRScope II infrared microscope (7000–15000 cm^{-1}). The room temperature infrared absorption spectrum of $LiSO_3CH_2SF_5$ was recorded as a reference.

The frequency-dependent optical conductivity was calculated by means of the Kramers-Krönig analysis of the measured reflectance. The range of data outside the

*Intermolecular contacts shorter than the sum of the sulfur van der Waals radii.

middle infrared was extended using 300 K spectra, for all the temperatures. The high frequency data were extrapolated as ω^{-2}, where ω is the frequency, and the low frequency data were extrapolated as a constant appropriate for semiconducting materials [5]. Complex vibrational bands were analysed using standard peak fitting techniques to extract centre peak frequencies and integral areas (oscillator strengths). Oscillators were fitted using the Voigt function*.

3. Results and discussion

Figure 1 displays the optical conductivity spectra of β″-(ET)$_2$SF$_5$CH$_2$SO$_3$ recorded at 10 and 300 K, together with the 300 K polarized reflectance (inset in Fig. 1a).

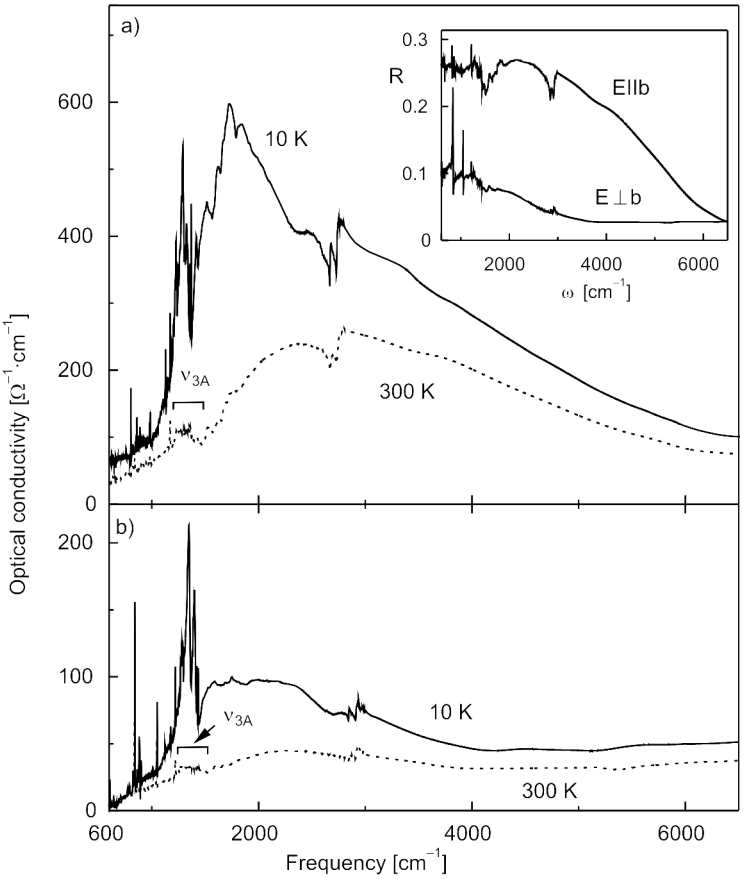

Fig. 1. Optical conductivity spectra of β″-(ET)$_2$SF$_5$CH$_2$SO$_3$ polarized in the $E \parallel b$ (a) and $E \perp b$ (b) directions, recorded at 10 and 300 K. The inset in Fig. 1a displays the polarized infrared reflectance at 300 K

*The Voigt function is a four-parameter model spectral line that includes two types of broadening, characteristic of both the Gaussian and Lorentzian shape.

The reflectance in the interstack direction ($E \parallel b$) is significantly greater than the reflectance in the stack direction ($E \perp b$) and displays a drop between 3000 and 6500 cm^{-1}. The reflectance spectrum polarized in the $\perp b$ direction is similar to the $E \parallel b$ response but is characterized by overdamping. Such a type of anisotropy is characteristic of a β″-phase quasi-two-dimensional conductor [1]. In fact, a similar behaviour is observed in the infrared spectra of β″-$(ET)_2SF_5CH_2CF_2SO_3$ superconductor and β″-$(ET)_2SF_5CHFSO_3$ metallic sample [3]. In the optical conductivity spectra of β″-$(ET)_2SF_5CH_2SO_3$, in both the $E \parallel b$ and $E \perp b$ polarizations (Fig. 1), one can observe at 300 K a broad electronic band centred near 2200 cm^{-1}. Upon lowering the temperature, this electronic excitation grows monotonically, slightly moves toward lower frequencies and displays a gap-like, low-frequency edge, probably related to the charge gap. Overall temperature changes in electronic excitation are modest, unlike vibrational structure.

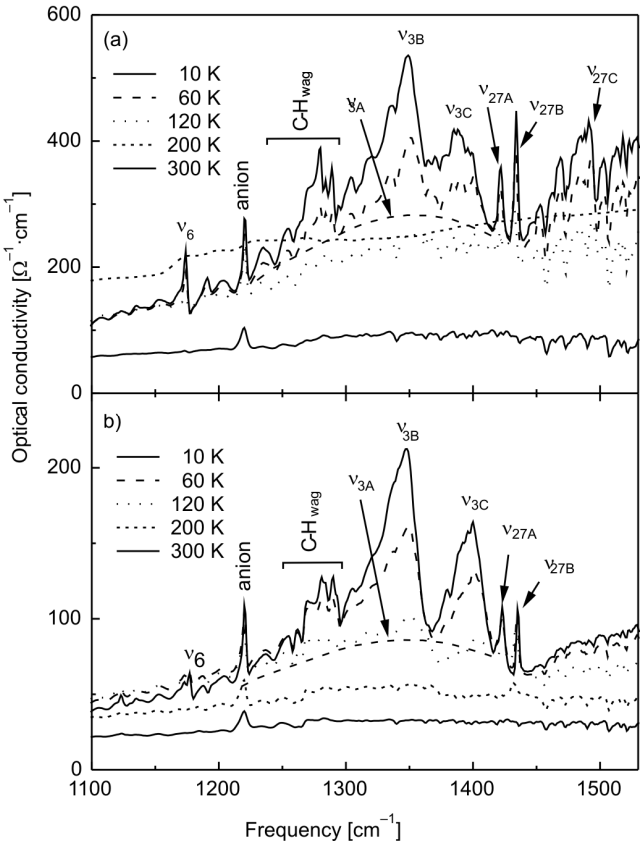

Fig. 2. Optical conductivity spectra of β″-$(ET)_2SF_5CH_2SO_3$ in the frequency range of the prominent vibrational features for $E \parallel b$ (a) and $E \perp b$ (b), measured at various temperatures

Figure 2 displays the optical conductivity spectra of β″-$(ET)_2SF_5CH_2SO_3$ in the range of the most prominent vibrational modes at various temperatures. In general, the

infrared spectra of ET-based materials mostly display intramolecular modes of the ET molecule, and the strongest features appear as a result of electron-molecular vibration (EMV) coupling of totally symmetric modes with electrons [6–8]. These so-called vibronic modes are infrared active in the presence of symmetry breaking, usually dimerization [9]. Unlike most ET-based solids, the spectra of β″-(ET)$_2$SF$_5$CH$_2$SO$_3$, at 300 K in the frequency range corresponding to vibrational features, are characterized by relatively strong modes of the SF$_5$CH$_2$SO$_3$ anion. For example, in the $E \perp b$ polarization, the anion modes are found at 841, 1050 and 1220 cm^{-1} (the 1220 cm^{-1} mode is shown in Fig. 2 for both polarizations). These modes do not change much upon lowering temperature. On the other hand, very strong ET-related modes grow upon lowering the temperature below about 250 K in both the polarizations (Fig. 2). In particular, the largest effect is observed in the frequency range 1300–1410 cm^{-1} for the totally symmetric bridge C=C stretching mode labelled $\nu_3(A_g)$ in the D_{2h} point group symmetry representation we use here for isolated molecule [7]. This mode having a large coupling constant [8] is known for its sensitivity to both structural as well as charge modifications [10]. Other prominent EMV-related effects observed in the spectra include C–H wagging vibrations (1250–1300 cm^{-1}), C–S stretching vibrations (870–910 cm^{-1}, see Fig. 3), and the $\nu_6(A_g)$ mode at about 1174 cm^{-1}. In addition, the out-of-phase stretching C=C mode $\nu_{27}(B_{1u})$ displays a similar behaviour although it is normally infrared active and not coupled based on the symmetry considerations. Most of the above mentioned features appear as multiple peaks. Another C=C stretching mode $\nu_2(A_g)$, which can appear in the infrared spectra as a result of coupling with electrons, is characterized by a small coupling constant [7], and for this reason it is absent in the infrared spectra of β″-(ET)$_2$SF$_5$CH$_2$SO$_3$.

The unit cell of the β″-(ET)$_2$SF$_5$CH$_2$SO$_3$ system is triclinic (space group $P\bar{1}$) and accommodates four ET donor molecules. Therefore, every internal ET vibration splits into four components, forming unit-cell modes. These modes should be fourfold degenerated in the case if four molecules in the unit cell are almost equivalent. In the β″-(ET)$_2$SF$_5$CH$_2$SO$_3$ material, there are molecules with two different values of charge present over the whole temperature range. As a result, we could expect at least two separate peaks to appear in the infrared spectra for each charge-sensitive mode, including $\nu_3(A_g)$ and also $\nu_{27}(B_{1u})$ [11]. To discuss vibrational features in a more detailed way, we use factor-group analysis, taking into account these two modes. In the factor-group symmetry C_i, four crystalline modes for both the $\nu_3(A_g)$ and $\nu_{27}(B_{1u})$ are split into two pairs of A_g and A_u modes, the two former being Raman active and the two latter being infrared active. This mutual exclusion rule is related to the inversion centre present in the $P\bar{1}$ space group. The $\nu_3(A_g)$ mode appears in the $E \parallel b$ and $E \perp b$ spectra of β″-(ET)$_2$SF$_5$CH$_2$SO$_3$ below 250 K, mainly as two very strong features (ν_{3B} and ν_{3C} in Fig. 2) centred at about 1348 and 1400 cm^{-1} at the lowest temperature. We assign these modes to two EMV-activated ungerade crystalline modes (A_u). Another very broad ν_3 component, labelled as $\nu_{3A,}$ appears in the frequency range 1200–1450 cm^{-1} (the dashed line marked in Fig. 2 for the lowest temperature 10 K) over the whole

temperature range (see spectra at 300 K in Fig. 1 for comparison). Such a broad but substantially stronger vibronic ν_3 feature is characteristic of infrared spectra of the β″-$(ET)_2SF_5RSO_3$ (R = CH_2CF_2, $CHFCF_2$, and CHF) family of materials including a superconductor (R = CH_2CF_2), a material with the metal/insulator phase transition (R = $CHFCF_2$) and a metallic sample (R = CHF) [3]. We suggest that this is the crystalline mode of the A_g symmetry that is supposed to be Raman active only. In fact, a strong low-frequency component of ν_3 was found at about 1330 cm^{-1}, in the 80 K Raman spectrum of the analogue material β″-$(ET)_2CF_3CH_2SO_3$ [12], and both in Raman and infrared spectra of the charge-ordered phase of θ-$(ET)_2RbZn(SCN)_3$ [10]. That it appears in the infrared spectra means that the inversion symmetry is broken in the β″-$(ET)_2SF_5CH_2SO_3$ material.

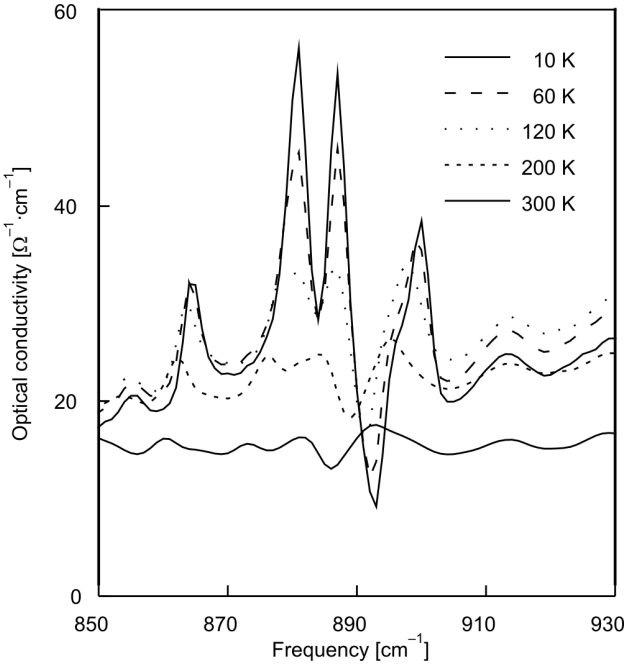

Fig. 3. Temperature dependence of intensity of selected vibrational C=C modes normalized by the 10 K values for β″-$(ET)_2SF_5CH_2SO_3$ (lines between points are intended to guide the eye)

Similarly to ν_3, the ν_{27} mode also displays three components: 1423, 1435, and ca. 1497 cm^{-1} at low temperatures, labelled as ν_{27A}, ν_{27B}, and ν_{27C} in Fig. 2, respectively. This mode is considered to be the best probe of the local charge on the molecule [11]. Here we assign the ν_{27A} and ν_{27B} components as related to the hole-rich molecules, and ν_{27C} as the mode belonging to the hole-poor molecules in the structure. When lowering the temperature, the ν_{27B} and ν_{27C} components appear in the infrared spectra at about 200 K, and the ν_{27A} mode is displayed at about 120 K. Using the linear relationship between the frequency and charge ρ on the molecule [11]

$$\nu_{27}(\rho) = 1398 + 140(1 - \rho)\ [\mathrm{cm}^{-1}]$$

and taking into account the ν_{27B}* and ν_{27C} components, we estimate the fractional charge in β″-(ET)$_2$SF$_5$CH$_2$SO$_3$ to be 0.3*e* and 0.7*e*. Our result is different from the values 0.4*e* and 0.6*e* calculated based on the bond lengths [4]. Other EMV coupling-related effects accompanied by mode splitting are observed for the C–H wagging vibrations in the frequency range 1250–1300 cm^{-1} (Fig. 2) and for the C–S stretching mode (ca. 880 cm^{-1}, Fig. 3) which is known to be strongly temperature dependent in the infrared spectra of ET-based organic conductors [13].

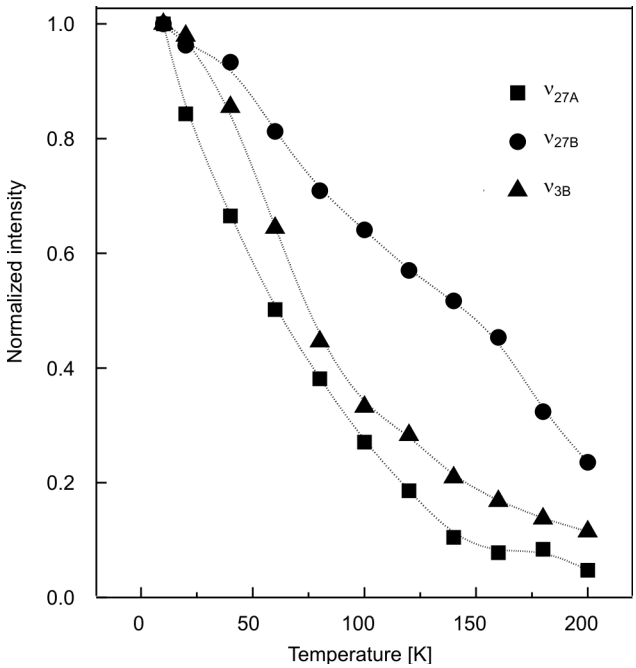

Fig. 4. Optical conductivity spectra of β″-(ET)$_2$SF$_5$CH$_2$SO$_3$ in the frequency range of the stretching C–S mode for polarization E ⊥ *b*, measured at selected temperatures

To discuss the temperature dependence of the ν_3 and ν_{27} mode components, we calculated the integral intensities (oscillator strengths) of ν_{27A}, ν_{27B} and ν_{3B} for the infrared spectra polarized in the *E* ∥ *b* direction. Figure 4 displays the temperature dependence of the selected mode intensities, normalized by the 10 K values. We have chosen these components because they are relatively strong and are not disturbed by an excessive noise. In the case of vibronic modes (i.e. modes activated through EMV coupling), the infrared oscillator strength is related to stack dimerization amplitude

*We have chosen ν_{27B} out of two low frequency ν_{27} components because it appears in broader temperature range than ν_{27A}.

[14, 15]. In fact, a very strong temperature dependence of the integral intensity of the ν_{3B} mode is observed for β″-$(ET)_2SF_5CH_2SO_3$. Such a behaviour suggests that the material undergoes apparent dimerization upon a lowering of temperature. Surprisingly, both the ν_{27} components grow proportionally to ν_3, and temperature dependence of integral intensity of ν_{27A} is even more steep than in the case of ν_3 (Fig. 4). The ν_{27B} mode is characterized by a weaker temperature dependence but it is still much stronger than in case of other normally infrared-active vibrations (see the anion mode in Fig. 2 for comparison). To explain this unusual behaviour, we suggest that EMV coupling is also involved in activation of the ν_{27} mode components. Probably, due to local symmetry of the ET donor molecule and factor-group splitting, the ν_{27} mode partly gains a new identity as a totally symmetric mode and hence is available for coupling with electrons.

Although β″-$(ET)_2SF_5CH_2SO_3$ does not undergo any phase transition in the studied temperature range, the vibronic signatures of dimerization observed in this material are very strong and include factor-group splitting. We suggest that hydrogen bonding between anion layer and ET donor layer takes part in dimerization providing a mechanism for strong interaction between ET molecules.

4. Conclusions

The polarized infrared spectra of β″-$(ET)_2SF_5CH_2SO_3$ were recorded at various temperatures. The material is a two-dimensional semiconductor, with an electronic response similar to that of the β″-$(ET)_2SF_5RSO_3$ (R = CH_2CF_2, $CHFCF_2$, and CHF) family of materials. The vibrational study reveals a very strong activation and splitting of the ν_3 and ν_{27} modes as the temperature is lowered. We suggest that these effects are related both to EMV coupling within the dimerized structure and to the presence of two different charges on ET molecules in the donor layer. Unusually strong temperature dependence of all the vibronic signatures of dimerization indicates that hydrogen bonding between anions and donor molecules facilitates stabilization of ET dimers at low temperature.

Acknowledgement

This work was supported by the Ministry of Science and Higher Education of Poland as the research project in the years 2008–2010.

References

[1] SEO H., HOTTA C., FUKUYAMA H., Chem. Rev., 104 (2004), 5005.

[2] OLEJNICZAK I., JONES B.R., ZHU Z., DONG J., MUSFELDT J.L., SCHLUETER J.A., MORALES E., GEISER U., NIXON P.G., WINTER R.W., GARD G.L., Chem. Mater., 11 (1999), 3160.

[3] JONES B.R., OLEJNICZAK I., DONG J., PIGOS J.M., ZHU Z.T., GARLACH A.D., MUSFELDT J.L., KOO H.-J., WHANGBO M.-H., SCHLUETER J.A., WARD B.H., MORALES E., KINI A.M., WINTER R.W., MOHTASHAM J., GARD G.L., Chem. Mater., 12 (2000), 2490.

[4] WARD B.H., SCHLUETER J.A., GEISER U., WANG H.H., MORALES E., PARAKKA J.P., THOMAS S.Y., WILLIAMS J.M., NIXON P.G., WINTER R.W., GARD G.L., KOO H.-J., WHANGBO M.-H., Chem. Mater., 12 (2000), 343.
[5] WOOTEN, F., *Optical Properties of Solids*, Academic Press, New York, 1972.
[6] RICE M.J., Phys. Rev. Lett., 37 (1976), 36.
[7] KOZLOV M.E., POKHODNIA K.I., YURCHENKO A.A., Spectrochim. Acta, 43A (1987), 323.
[8] GIRLANDO A., MASINO M., BRILLANTE A., DELLA VALLE R.G., VENUTI E., *Pairing mechanism in organic superconductors: the entangled role of phonons*, [in:] Ross W. Stevens (Ed.), *New Developments in Superconductivity Research*, Nova Science Publishers, New York 2003, p. 15.
[9] MENEGHETTI M., BOZIO R., PECILE C., J. Physique (France), 47 (1986), 1377.
[10] YAMAMOTO K., YAKUSHI K., MIYAGAWA K., KANODA K., KAWAMOTO A., Phys. Rev. B, 65 (2002), 085110.
[11] YAMAMOTO T., URUICHI M., YAMAMOTO K., YAKUSHI K., KAWAMOTO A., TANIGUCHI H., J. Phys. Chem. B, 109 (2005), 15226.
[12] WOJCIECHOWSKI R., unpublished results.
[13] MUSFELDT J.L., ŚWIETLIK R., OLEJNICZAK I., ELDRIDGE J.E., GEISER U., Phys. Rev. B, 72 (2005), 014516.
[14] RANZIERI P., MASINO M., GIRLANDO A., LEMÉE-CAILLEAU M.-H., Phys. Rev. B, 76 (2007), 134115.
[15] PAINELLI A., DEL FREO L., SOOS Z.G., Synth. Met., 133-134 (2003), 619.

Received 10 July 2008
Revised 15 September 2008